Development 133, 2661-2669 (2006) doi:10.1242/dev.02435

Moz-dependent Hox expression controls segment-specific fate maps of skeletal precursors in the face

Justin Gage Crump*, Mary E. Swartz, Johann K. Eberhart and Charles B. Kimmel

Development of the facial skeleton depends on interactions between intrinsic factors in the skeletal precursors and extrinsic signals in the facial environment. Hox genes have been proposed to act cell-intrinsically in skeletogenic cranial neural crest cells (CNC) for skeletal pattern. However, Hox genes are also expressed in other facial tissues, such as the ectoderm and endoderm, suggesting that Hox genes could also regulate extrinsic signalling from non-CNC tissues. Here we study *moz* mutant zebrafish in which *hoxa2b* and *hoxb2a* expression is lost and the support skeleton of the second pharyngeal segment is transformed into a duplicate of the first-segment-derived jaw skeleton. By performing tissue mosaic experiments between *moz*$^{-}$ and wild-type embryos, we show that Moz and Hox genes function in CNC, but not in the ectoderm or endoderm, to specify the support skeleton. How then does Hox expression within CNC specify a support skeleton at the cellular level? Our fate map analysis of skeletal precursors reveals that Moz specifies a second-segment fate map in part by regulating the interaction of CNC with the first endodermal pouch (p1). Removal of p1, either by laser ablation or in the *itga5*^{b926} mutant, reveals that p1 epithelium is required for development of the wild-type support but not the *moz*$^{-}$ duplicate jaw-like skeleton. We present a model in which Moz-dependent Hox expression in CNC shapes the normal support skeleton by instructing second-segment CNC to undergo skeletogenesis in response to local extrinsic signals.

KEY WORDS: Craniofacial, Skeleton, Zebrafish, Moz, Hox, Morphogenesis

INTRODUCTION

Hox genes regulate organ identity along the anteroposterior axis (Hombria and Lovegrove, 2003), yet how Hox genes control segment-specific organ shape at the cellular level is poorly understood. The vertebrate facial skeleton is derived from cranial neural crest cells (CNC) arranged into a series of segments, or 'arches', of the pharynx (Le Douarin, 1982). In zebrafish, CNC of the second (hyoid) segment express *hoxa2b* and *hoxb2a* and generate the support skeleton for the jaw and gill cover, whereas first (mandibular) segment CNC do not express Hox genes and generate the jaw skeleton (Hunt et al., 1991; Schilling and Kimmel, 1994). In diverse vertebrates, loss of the Hox2 genes, *Hoxa2* or *hoxa2b/hoxb2a*, causes a mirror-image duplication of the jaw skeleton to form in the second segment (Gendron-Maguire et al., 1993; Hunter and Prince, 2002; Miller et al., 2004; Rijli et al., 1993). In a reciprocal manner, forced expression of *Hoxa2* throughout the first segment causes partial transformation of the jaw skeleton toward a second-segment skeletal morphology (Grammatopoulos et al., 2000; Hunter and Prince, 2002; Pasqualetti et al., 2000).

moz encodes a histone acetyltransferase required to maintain Hox expression in the hindbrain and in postmigratory CNC and epithelia of the second segment (Fig. 1) (Miller et al., 2004). In wild-type larvae, the first-segment-derived skeleton includes Meckel's (M) and palatoquadrate (Pq) cartilages, which form the primary lower and upper jaw elements, respectively. The second-segment-derived support skeleton includes the ceratohyal (Ch) cartilage, the hyosymplectic (Hs) cartilage [composed of hyomandibular (Hm) and symplectic (Sy) elements], which bridges the upper jaw to the ear, and opercular (Op) and branchiostegal ray (Br) dermal bones, which support the gill cover (Fig. 2A). In *moz* mutants, second-segment support cartilages are replaced by an extra set of jaw-like cartilages, M-like (M') and Pq-like (Pq'), and second-segment dermal bones are lost (Fig. 2B) (Miller et al., 2004). This 'homeotic' phenotype resembles that seen in zebrafish with *hoxa2b* and *hoxb2a* function reduced by morpholinos [Fig. 2C and Hunter and Price (Hunter and Prince, 2002); hereafter referred to as *hox2*-MO animals]. We chose to focus our study on the *moz* mutant for several reasons. First, the *moz* mutant phenotype is more consistently expressive than the phenotype seen in *hox2*-MO larvae. Second, whereas Moz is required for the maintenance of Hox expression in postmigratory CNC, Moz is not required for earlier Hox expression at premigratory stages (Miller et al., 2004). Because early Hox expression and neural crest induction and migration are normal in *moz* mutants, studying *moz* allows us to selectively probe the postmigratory functions of Hox genes in skeletal patterning.

Moz is required not only for *hoxa2b* and *hoxb2a* expression in second-segment CNC but also for *hoxa2b* expression in a subset of ectoderm and endoderm that surrounds second-segment CNC (this work) (Miller et al., 2004). It is clear from studies in chicken, zebrafish and mouse that signals from the ectoderm and endoderm pattern the CNC-derived facial skeleton (Couly et al., 2002; Crump et al., 2004a; Crump et al., 2004b; Eberhart et al., 2006; Helms and Schneider, 2003; Piotrowski and Nusslein-Volhard, 2000; Ruhin et al., 2003). Although Hox2 genes are expressed in the ectoderm and endoderm, the skeletal patterning function of Hox2 expression in these tissues has not been directly tested. Using tissue mosaic experiments in zebrafish, in which we selectively restored or removed Moz or Hoxa2b/Hoxb2a function from specific facial tissues, we demonstrate that Moz and Hox2 genes function in CNC, but not in the ectoderm or endoderm, for patterning of the second-segment-derived skeleton. Next, we used single cell labelling and time-lapse analysis to show that Moz specifies the fate map of second-segment skeletal precursors. In particular, dorsal second-segment CNC, which form part of the Hs cartilage and Op dermal bone in wild type, fail to undergo skeletal differentiation in *moz* mutants, effectively positioning the duplicate jaw-like skeleton more

Institute of Neuroscience, 1254 University of Oregon, Eugene, OR, USA.

*Author for correspondence (e-mail: gage@uoneuro.uoregon.edu)

Accepted 9 May 2006

ventrally. Additionally, whereas p1 endoderm is crucial for normal Hs cartilage development (Crump et al., 2004b), the *moz*⁻ jaw-like cartilage (Pq') that replaces Hs does not require p1. We conclude that an important CNC-intrinsic function of Moz is to confer competence on skeletogenic CNC to respond to spatially restricted endodermal, and perhaps ectodermal, signals. Hence, normal Moz-dependent Hox expression determines where in the second segment skeletal differentiation occurs, thus establishing the spatial geometry of a support skeleton.

MATERIALS AND METHODS

Zebrafish strains

Zebrafish (*Danio rerio*) were raised at 28.5°C. *fli1*:GFP, *moz*^{b719} and *itga5*^{b926} strains are as described (Crump et al., 2004b; Lawson and Weinstein, 2002; Miller et al., 2004). In the construction of the *moz; fli1*:GFP strain we discovered that *fli1*:GFP and *moz* were tightly linked on LG5 (2/100 recombinants from a *moz* × *fli1*:GFP cross). Once constructed, the brighter fluorescence of homozygous *moz*; *fli1*:GFP embryos allowed us to greatly enrich for *moz* mutants at 24 hours postfertilization (hpf).

Phenotypic analysis

Facial skeletons were stained with Alcian Green, and flat mount dissections were performed as described (Crump et al., 2004a; Crump et al., 2004b). Whole-mount in-situ hybridization and the *hoxb2a* probe are as described (Miller et al., 2004). As the previously described *hoxa2b* probe (Miller et al., 2004) was found to cross-react with *fli1*:GFP, we used gene-specific primers containing the T3 promoter to amplify and synthesize the probe. Primers used were 5′: ACCCTGGTCCACTATACTTC and 3′: CGCGCAATTAACCCTCACTAAAGGGGAAATCAAAGGCCTCCGTA-G. For frozen sections, larvae were embedded in a mixture of 0.9% agar, 1% low melt agarose and 5% sucrose, frozen by suspension above liquid nitrogen, and cut at 16-μm intervals with a Leica CM3050S cryotome. In-situ hybridization was then performed on frozen sections as described (Rodriguez-Mari et al., 2005). *hoxa2b*-MO and *hoxb2a*-MO were injected together into 1-cell embryos at 5 mg/ml each in a 3-nl volume (Miller et al., 2004).

Transplants and microelectroporation

Alexa-568-labelled CNC, endoderm and neural precursors were transplanted at shield stages as described (Crump et al., 2004a; Crump et al., 2004b). The transplant technique for facial surface ectoderm precursors was similar to that described for CNC transplants (Crump et al., 2004b), except that donor ectoderm was placed 120° from dorsal and midway between the margin and animal pole of host embryos at shield stage. All transplants were unilateral, and, except where indicated otherwise, both donors and hosts harboured *fli1*:GFP. For CNC, ectoderm and endoderm transplants, animals were selected for analysis if donor tissue constituted at least half of second-segment CNC, ectoderm or endoderm based on inspection in a fluorescence dissecting microscope. Microelectroporations were performed as described (Crump et al., 2004b; Lyons et al., 2003). Each point represents a cell or the centroid of a pair of cells in an individual. Lateral and dorsal cross-sectional views were made at the level of labelled cells using Zeiss LSM software and plotted onto schematics of generalized pharyngeal segments.

Laser ablation

The first endodermal pouch was ablated using high-power laser irradiation. In order to visualize laser irradiation, *fli1*:GFP or *moz*; *fli1*:GFP embryos were injected with RNA encoding for the Kaede photoconvertible fluorescent protein (Ando et al., 2002) at the one-cell stage. At 28-32 hpf, embryos were mounted in 0.2% agarose and, using a Biorad Radiance 2100 multi-photon microscope, a preliminary scan was performed to localize p1. Then, using the ROI tool of the Biorad Lasersharp software to select only p1, we irradiated p1 for 5 minutes with a 10 W Millenia/Tsunami (Spectraphysics) laser tuned to 780 nm and at 100% power. Scans taken immediately after irradiation showed that the Kaede protein was efficiently converted to red emission specifically in p1 (data not shown). Embryos were re-imaged 4 hours post-irradiation using Nomarski polarization and fixed at 5 days postfertilization (dpf) for Alcian staining. In approximately half of irradiated animals, Nomarski imaging revealed that p1 cells were visibly damaged compared with neighbouring unirradiated cells. In a fraction of animals, p1 cells did not appear damaged and no cartilage defects were observed. Thus, we only used animals in which p1 was visibly damaged for our skeletal analysis.

Microscopy

Digital images of facial skeletons and in situ hybridization were obtained on a Zeiss Axiophot 2 microscope using Axiocam software. Levels were uniformly adjusted using Adobe Photoshop CS2 software. Fluorescent imaging and time-lapse recordings were done on a Zeiss LSM5 Pascal confocal microscope as described (Crump et al., 2004b). Except when indicated otherwise, anterior is to the left and ventral is down in all panels.

RESULTS

Limited expression of second-segment Hox genes outside CNC

In order to address how Hox2 genes specify second-segment skeletal morphology, a detailed understanding of second-segment Hox2 expression is essential. However, the facial expression of *Hoxa2* in mouse and chicken (Couly et al., 1998; Hunt et al., 1991; Maconochie et al., 1999) and *hoxa2b* and *hoxb2a* in zebrafish (Hunter and Prince, 2002; Miller et al., 2004) are less well characterized outside the CNC. Hence, we examined *hoxa2b* and

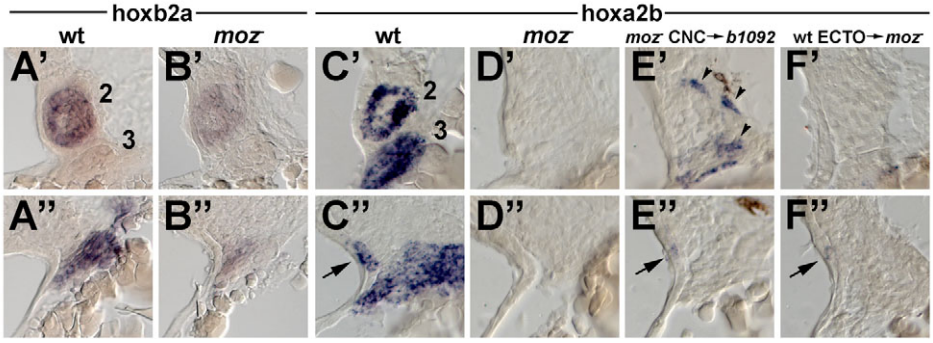

Fig. 1. Moz is required for Hox expression in multiple facial tissues. Horizontal sections were taken at 34 hpf at dorsal (A′-F′) and ventral (A″-F″) levels of the pharyngeal segments and stained with probes against *hoxb2a* (**A**,**B**) or *hoxa2b* (**C**-**F**). The second and third segments (numbered) from individual sides are shown with anterior to the top and lateral (ectoderm) to the left. (**A′**,**A″**) In the wild-type pharynx, *hoxb2a* is expressed exclusively in CNC of the second segment. (**B′**,**B″**) *hoxb2a* expression is very reduced in *moz* mutants. (**C′**,**C″**) In wild types, *hoxa2b* is strongly expressed in the CNC of the second and more posterior segments but not in the mesoderm core of the second segment. Ventral sections show additional expression in a small amount of surface ectoderm (arrows). In other sections, *hoxa2b* expression is seen in the endoderm of the second and more posterior pouches (data not shown). (**D′**,**D″**) In *moz* mutants, *hoxa2b* expression is absent or very reduced in CNC, surface ectoderm and endoderm. (**E′**,**E″**) In *b1092* mutant sides that received *moz*⁻ CNC transplants (see text), *hoxa2b* expression is lost in CNC. In this example, a small amount of CNC expression persists (arrowheads). However, weak expression of *hoxa2b* in the ectoderm is still seen (arrow). (**F′**,**F″**) In *moz*⁻ sides that received wild-type ectoderm transplants (see text), *hoxa2b* expression is present in the ectoderm (arrow) but absent in CNC.

hoxb2a expression in horizontal sections of zebrafish larvae at 34 hpf, a time after CNC migration (11-18 hpf) but before the first skeletogenesis (52 hpf) (Fig. 1A,C). In accord with previous whole-mount analysis (Hunter and Prince, 2002; Miller et al., 2004), sections show that both *hoxa2b* and *hoxb2a* are expressed in postmigratory CNC. In addition, *hoxa2b*, but not *hoxb2a*, is expressed in a small region of ventral ectoderm extending from the anterior portion of the second pharyngeal segment into the first segment. This ectodermal expression appears similar to that described for mouse *Hoxa2* (Maconochie et al., 1999). However, we did not detect widespread expression of *hoxa2b* or *hoxb2a* in second-segment ectoderm. In the endoderm, *hoxa2b*, but not *hoxb2a*, was expressed in the second pouch but not in the first pouch or endoderm medial to second-segment CNC. Thus, as reported for *Hoxa2* in other vertebrates, zebrafish *hoxa2b* is expressed in a very limited pattern in the pharyngeal ectoderm and endoderm, and *hoxb2a* pharyngeal expression is restricted to CNC. Lastly, we found *hoxa2b* and *hoxb2a* expression to be either absent or very reduced in the CNC, ectoderm, and endoderm of *moz*$^{-}$ larvae (Fig. 1B,D).

Moz functions in CNC to specify a support skeleton

As we found Hox2 expression in tissues outside the CNC, we asked whether Moz and Hox2 genes function exclusively in CNC or additionally in other head tissues for skeletal patterning. In order to test if Moz is sufficient in CNC to restore normal skeletal patterning to *moz* mutants, we transplanted wild-type CNC precursors into *moz*$^{-}$ hosts. In transplants where donor wild-type CNC populated a large proportion of the second segment, we found that wild-type CNC formed a wild-type support skeleton in otherwise *moz*$^{-}$ hosts (Fig. 2E-L). Indeed, wild-type CNC restored both normal cartilage (Hm, Sy, Ch) and dermal bone (Op, Br) development to *moz*$^{-}$ hosts. Strikingly, in transplants with fewer donor cells, *moz*$^{-}$ CNC tended to sort to the anterior, ventral region of the mosaic second segment (Fig. 2I-L). In these cases, we observed hybrid cartilage patterns in which wild-type CNC formed support cartilage and *moz*$^{-}$ CNC formed jaw-like cartilage in the same segment. The strict CNC autonomy of the *moz*$^{-}$ phenotype suggests that individual or small groups of CNC interpret the presence of Moz independently and differentiate accordingly.

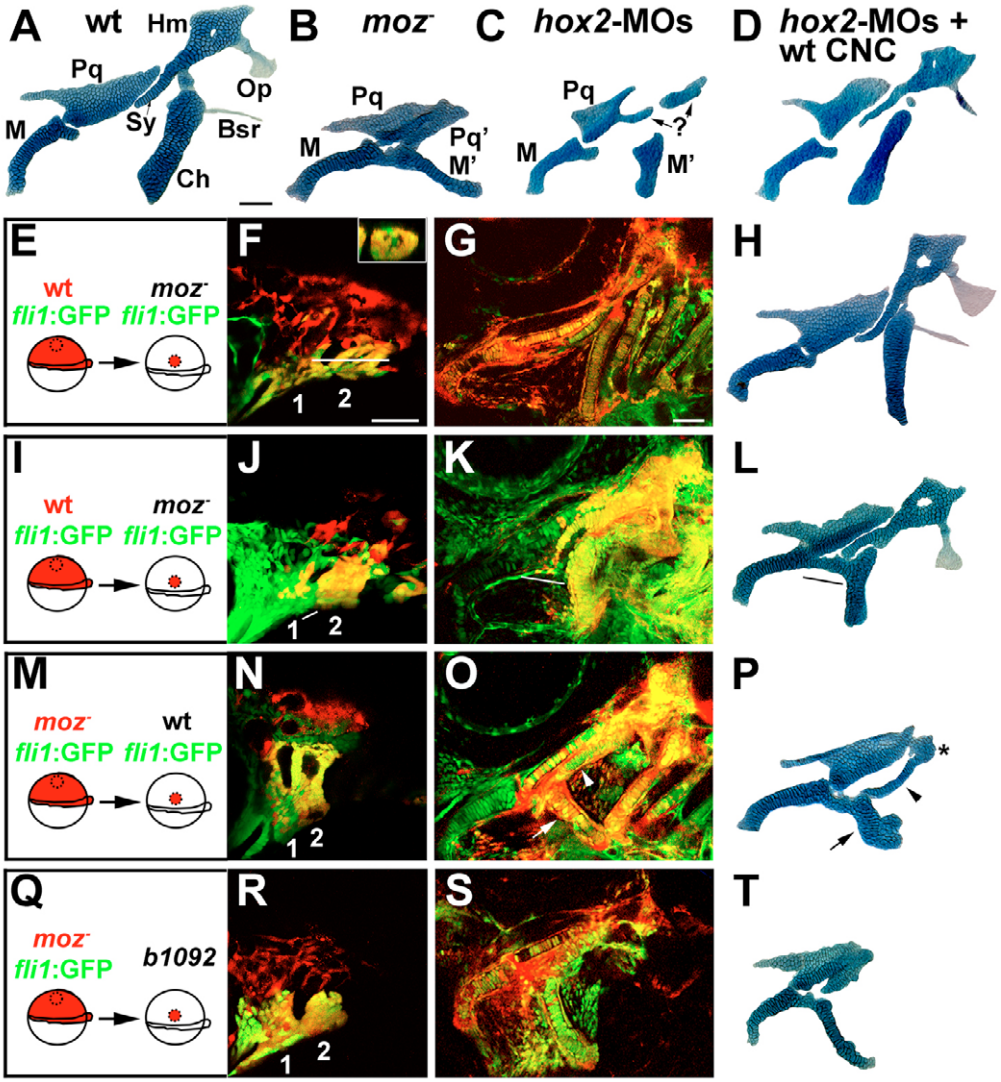

Fig. 2. Moz and Hox2 genes function in CNC to control second-segment skeletal identity. (A-D,H,L,P,T) Facial skeletons from 4 dpf larvae. (**A**) Wild type. (**B**) *moz*$^{-}$ control side of H. (**C**) *hox2*-MO animal (control side of D). (**D**) *hox2*-MO animal unilaterally rescued with wild-type CNC. (**E**,**I**) Schematics showing unilateral transplantation of wild-type CNC precursors (red) into *moz*$^{-}$ hosts. *fli1*:GFP labels all CNC green. Wild-type CNC (red) populate the second segment (2) at 32 hpf (**F**,**J**) and by 4 dpf (**G**,**H**,**K**,**L**) form largely normal Hm, Sy, Ch, Op and Br skeletal elements in 8/10 *moz*$^{-}$ hosts. Inset in F is a digital longitudinal section through the white line and shows co-localization of the transplant lineage tracer and the *fli1*:GFP. Lateral is up. In I-L, a hybrid skeleton was observed. In this example, M′-like (black line in L) and Ch cartilages were fused together, with M′ consisting of *moz*$^{-}$ host CNC (white lines in J and K), and Hm, Sy and Ch cartilages and Op osteocytes consisting entirely of wild-type donor CNC. (**M**) Schematic of transplantation of *moz*$^{-}$ CNC (red and green) into wild-type hosts. Both donor and host are *fli1*:GFP^{+}. (**N**) *moz*$^{-}$ CNC (red) populate the second segment (2) at 36 hpf. (**O**,**P**) At 4 dpf, partial PQ′-like (*) and M′-like (arrow) cartilages consist of *moz*$^{-}$ donor CNC (white arrow), and a Sy-like element (arrowheads) forms primarily from wild-type host CNC. In 9/10 cases, *moz*$^{-}$ CNC precursors formed jaw-like cartilages in a wild-type host. (**Q**) Schematic of transplantation of *moz*$^{-}$*; fli1*:GFP CNC (red and green) into *b1092* hosts (note that hosts are *fli1*:GFP^{-}). *moz*$^{-}$ CNC populate the first two segments (1,2) at 32 hpf (**R**) and by 4 dpf form *moz*$^{-}$-like M′ and Pq′ cartilages (**S**,**T**) in 6/9 *moz*$^{+}$ hosts. Scale bars: 50 μm.

The rescue of *moz*⁻ skeletal transformations by wild-type CNC shows that Moz need only be functional in second-segment CNC for a normal support skeleton to develop. In order to test if Moz is required in CNC for support skeletal development, we transplanted *moz*⁻ CNC precursors into wild-type hosts to generate animals in which Moz is selectively lost in CNC. When we examined animals in which a large proportion of the second segment consisted of *moz*⁻ CNC, the support skeleton was largely transformed into a jaw-like character (Fig. 2M-P), similar to that seen in fully *moz*⁻ animals. Further analysis suggested that the lack of a complete transformation was due to remaining wild-type CNC in the second segment. In order to create animals in which the entire second segment was populated by *moz*⁻ CNC, we made use of a newly discovered mutant, *b1092*. Homozygous *b1092* mutants lack all CNC-derived skeletal elements due to a defect in CNC generation, and this defect is completely rescued by wild-type CNC transplants (J.G.C., unpublished). When instead of wild-type CNC we transplanted *moz*⁻ CNC into *b1092* mutants, we observed that second segments of normal appearance formed early (Fig. 2Q,R) and *hoxa2b* expression was lost in second-segment CNC (Fig. 1E). In these 'rescued' *moz*⁻ second segments, we observed transformed jaw-like skeletons, indistinguishable from those seen in fully *moz*⁻ animals (Fig. 2S,T). Thus, the function of Moz in CNC is both necessary and sufficient to explain all the facial skeleton defects seen in *moz* mutants.

Our results from CNC transplants suggest that Moz has no skeletal patterning functions in non-CNC tissues. In order to examine functions of Moz directly in the ectoderm, endoderm and neural tube, we tested whether wild-type transplants of each of these tissues could restore normal skeletal development to *moz*⁻ hosts (Fig. 3). We used high-resolution confocal imaging to confirm that wild-type donor cells were targeted to individual tissues (Fig. 3), and for wild-type ectoderm transplants we verified that *hoxa2b* was expressed in the ectoderm but not the CNC of *moz*⁻ hosts (Fig. 1F). However, we found that transplants of wild-type ectoderm, endoderm or neural tube precursors were unable to rescue *moz*⁻ skeletal transformations. Thus, we do not detect a role for ectodermal and endodermal *hoxa2b* expression in patterning the support skeleton.

Hox genes are CNC-autonomous effectors of Moz in facial skeletal patterning

Previous analysis of *moz* mutants strongly suggested that Moz regulates skeletal patterning through the regulation of Hox2 genes: *hoxa2b* and *hoxb2a* expression are lost in *moz* mutants and the knockdown of *hoxa2b* and *hoxb2a* largely phenocopies the homeotic transformations seen in *moz* (Hunter and Prince, 2002; Miller et al., 2004). Thus, we tested whether Hox2 function, like Moz, is also sufficient in CNC to specify a support skeleton. In order to create embryos in which Hox2 function is eliminated in all tissues except CNC, we transplanted wild-type CNC precursors into *hox2*-MO larvae (Fig. 2C,D). Upon skeletal analysis, we observed that wild-type CNC fully rescued *hox2*-MO skeletal transformations. Thus, Hox2 genes need only be functional in CNC for support skeleton development.

In addition, we tested whether Moz regulates Hox2 expression cell-autonomously. Using wild type to *moz*⁻ and *moz*⁻ to wild type CNC transplants, we created second segment mosaics for wild-type and *moz*⁻ CNC and then examined these segments for *hoxb2a* expression (Fig. 4). We found a striking positive correlation between *hoxb2a* expression and the localization of wild-type CNC in the mosaic segments. Interestingly, we frequently observed a spatial segregation of wild-type and *moz*⁻ CNC, with *moz*⁻ CNC occupying more ventral and anterior regions. Thus, whereas in fully *moz*⁻ animals CNC can occupy the entire second segment, our mosaic experiments suggest that there may be adhesive differences between wild-type and *moz*⁻ CNC that are revealed by competition.

Moz controls the fate map of skeletal precursors

As we determined that Moz functions in CNC, we next examined how Moz functions at the cellular level to specify a particular skeletal arrangement. A prominent difference between the jaw and support skeleton is the dorsoventral location of the upper elements in their respective segments, required because the support but not the jaw skeleton of zebrafish attaches to the otic skeleton above (Fig. 2A; here we define ventral as where CNC contact the yolk, and dorsal as the upper limit of p1). Moz could regulate support versus jaw skeleton morphology either by instructing 'segmentally equivalent' skeletogenic CNC in similar regions of their respective

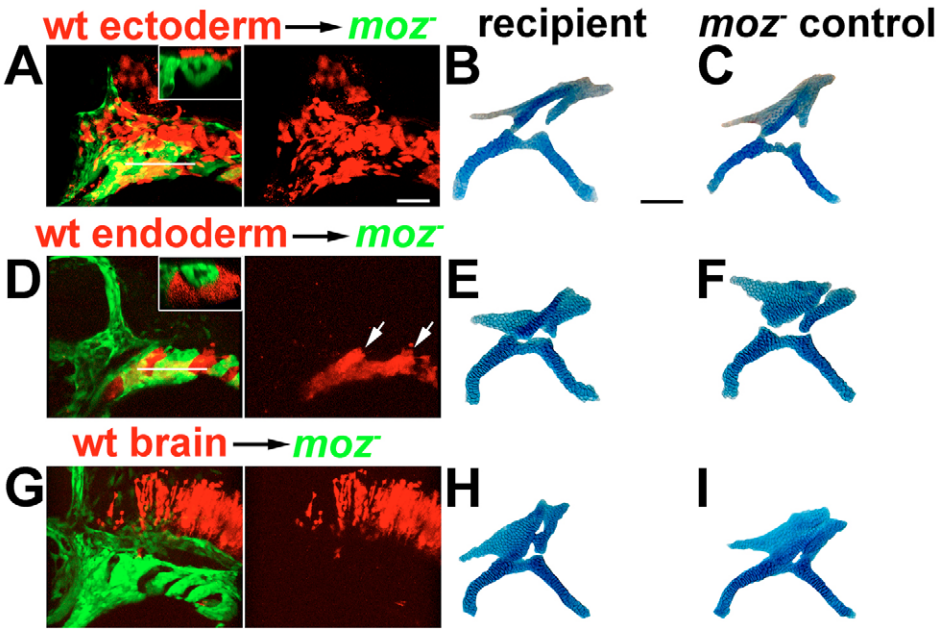

Fig. 3. Moz is not sufficient in the endoderm, surface ectoderm or hindbrain to rescue *moz*⁻ skeletal development. Wild-type ectoderm (**A-C**), endoderm (**D-F**) and hindbrain (**G-I**) precursors from *fli1*:GFP animals were unilaterally transplanted into *moz*⁻; *fli1*:GFP hosts at shield stage. Confocal images show that transplants (red) contributed significantly to the surface ectoderm (A), facial endoderm and pouches (arrows in D), and hindbrain (G) at 36 hpf. Insets in A and D are digital longitudinal sections through the level of the white lines and show that transplanted tissue did not express the *fli1*:GFP CNC marker. Lateral is up. (B,C,E,F,H,I) Facial skeletons of the first two segments from the transplanted animals at 4 dpf. Cartilages from the sides receiving transplants (B,E,H) were indistinguishable from the contralateral control sides (C,F,I). No rescue was seen in 3 ectoderm, 9 endoderm and 12 brain transplants. Scale bars: 50 μm.

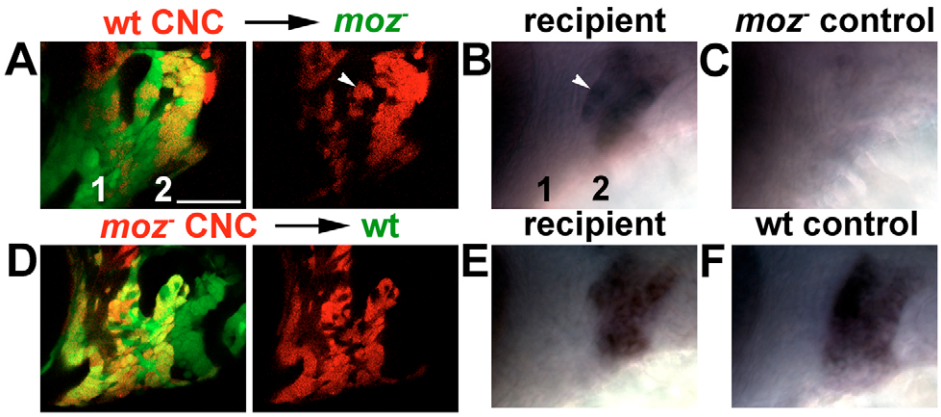

Fig. 4. Moz controls *hoxb2a* expression cell-autonomously in CNC. (**A**,**D**) Confocal images at 36 hpf of the first two segments (numbered in A) of *fli1*:GFP hosts after unilateral transplantation of CNC precursors (red) at shield stage. After live imaging, the same animals were fixed and stained with *hoxb2a* RNA probe. The transplant recipient sides (**B**,**E**) and the contralateral control sides that received no transplant (**C**,**F**) are shown. (A-C) Wild-type CNC in a *moz*⁻; *fli1*:GFP host cell-autonomously rescue *hoxb2a* expression in the second segment. Note the similar zones of red donor and *hoxb2a*-expressing CNC in A and B; white arrowheads denote a small group of isolated CNC rescued for *hoxb2a* expression. Second segments of control *moz*⁻ sides do not express *hoxb2a* (C). (D-F) *moz*⁻ CNC in a wild-type *fli1*:GFP host cell-autonomously fail to express *hoxb2a* in the second segment. Note the reciprocal zones of red donor and *hoxb2a*-expressing CNC in D and E. Second segments of control wild-type sides express *hoxb2a* (F). The similarity of *hoxb2a* expression in B and E shows that non-*hoxb2a*-expressing cells preferentially sort to the anterior ventral domain of the second segment. Scale bar: 50 μm.

segments to undergo different morphogenesis, or, alternatively, by controlling where in the segments skeletogenic differentiation occurs. In order to distinguish between these possibilities, we used single cell microelectroporation to make detailed fate maps of wild-type and *moz*⁻ skeletal precursors (Lyons et al., 2003). We extend our previous work (Crump et al., 2004b; Eberhart et al., 2006) and present here a fate map of wild-type animals at 24 hpf that includes cartilage (chondrocyte) precursors of the first two segments and dermal bone (osteocyte) precursors of the second segment (Fig. 5; see Fig. S1 in the supplementary material). In the second segment, the anterior portion of the Hm cartilage, the uppermost element, arises from a dorsal CNC domain along p1 endoderm. The Sy cartilage derives from dorsoventrally intermediate CNC, also along p1, and a more ventral CNC domain, close to medial pharyngeal endoderm, gives rise to Ch. By contrast, Op and Br dermal bone precursors map to the lateral domain of the second segment, immediately below the surface ectoderm. In the first segment, precursors of the Pq cartilage, the uppermost element, are located in a dorsoventrally intermediate domain, and M precursors are located in the ventral domain. Thus, the differences in the dorsoventral extent of the normal jaw and support skeletons result from the first-segment upper element, Pq, deriving from dorsoventrally intermediate CNC and the second-segment upper element, Hm, deriving from dorsal CNC.

We next tested whether skeletal transformations in *moz* mutants were due to second-segment skeletal precursors adopting a first-segment-type fate map. Indeed, our fate map of *moz* mutants at 24 hpf revealed that CNC that contribute to the duplicate jaw-like cartilages Pq' and M' map to different positions within the second segment compared with precursors of the support skeleton (Fig. 5; see Fig. S1 in the supplementary material). Interestingly, as with the duplicated jaw-like cartilages, the altered second-segment fate map of *moz* mutants appears to be a mirror image of the wild-type first-segment fate map, with the axis of symmetry being at the border

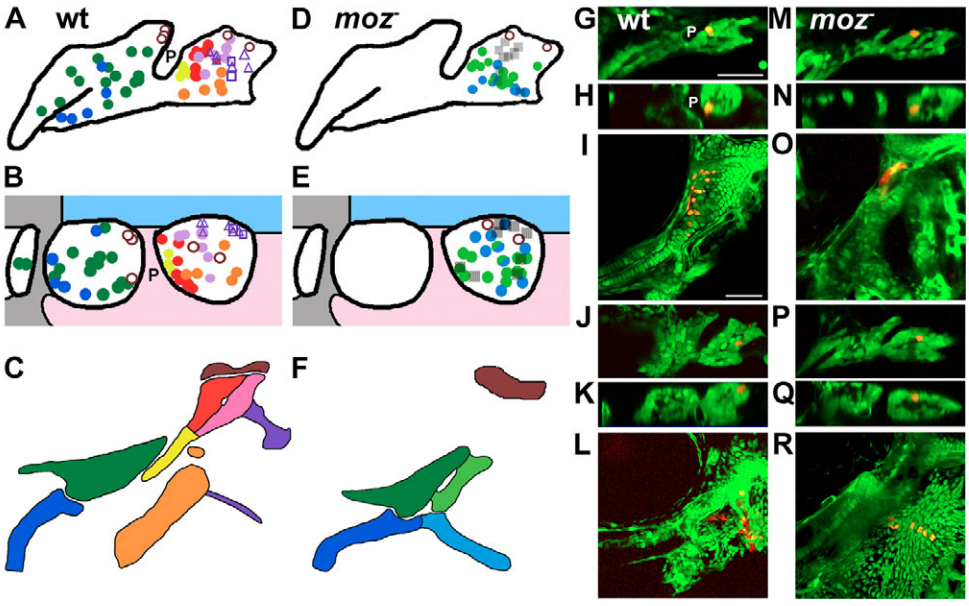

Fig. 5. The fate map of second-segment skeletal derivatives is altered in *moz* mutants. Summaries of wild-type (**A**-**C**) and *moz*⁻ (**D**-**F**) fate maps and representative examples (**G**-**R**). Lateral views (A,D,G,J,M,P) and dorsal cross-sectional views at the level of the labelled cell with anterior to the left and lateral up (B,E,H,K,N,Q) are shown at 24 hpf. The facial skeleton is shown at 4 dpf (C,F,I,L,O,R). Filled circles denote facial cartilage precursors, and open circles denote precursors of neurocranial cartilage that surrounds the otic capsule. Triangles and squares denote precursors of the Op (upper) and Br (lower) dermal bones, respectively. *moz*⁻ CNC that made no skeleton are hatched squares. In B and E, areas of surface ectoderm (blue), endoderm (pink), and stomodeal ectoderm (grey) are shown (compare to insets in Fig. 3A,D). In A,B,G,H, first pouch endoderm (P) is labelled. Wild-type examples of anterior Hm cartilage (G-I) and Op osteocyte (J-L) precursors are shown. (M-R) *moz*⁻ CNC in similar positions fail to make skeleton. Note that in both wild types and *moz* mutants the most dorsal CNC in the first and second segment contribute to neurocranial cartilage that surrounds the otic capsule. Scale bars: 50 μm.

between segments. In the *moz*⁻ second segment, CNC throughout the intermediate zone contributed to Pq' and more ventral CNC contributed to M'. However, *moz*⁻ CNC in the dorsal zone, including those along p1, did not contribute to the jaw-like cartilages by 5 dpf. This condition mimics that in the wild-type first segment, in which Hox genes are not normally expressed and dorsal CNC next to p1 do not form jaw cartilage. In addition, CNC in the lateral domain, which give rise to Op and Br bones in wild type, contribute instead to undifferentiated lateral mesenchyme in *moz*⁻ second segments, consistent with a lack of second-segment dermal bone in *moz* mutants. Thus, although there is considerable overlap between the *moz*⁻ and wild-type fate maps, we show that when Hox expression is lost in the *moz*⁻ second segment, precursors of dorsal facial cartilage and lateral bone fail to undergo skeletal differentiation.

Moz is required for the development of cartilage precursors adjacent to p1

As second-segment CNC along dorsal p1 endoderm fail to make cartilage in *moz* mutants, we made time-lapse recordings of wild-type and *moz*⁻ skeletal development to further examine the Moz-dependent interaction of dorsal cartilage precursors with p1. In the wild-type example, CNC are doubly labelled by *fli1*:GFP (Lawson and Weinstein, 2002) and mosaic transplantation of dye-labelled CNC (Fig. 6A; see Movie 1 in the supplementary material). As we reported previously (Crump et al., 2004b), in the wild-type second segment, dorsal CNC adjacent (and posterior) to p1 at 36 hpf form the anterior half of the Hm cartilage by 84 hpf. By contrast, in the first segment, dorsal CNC adjacent (and anterior) to p1 do not contribute to jaw cartilage by 84 hpf. Instead, in agreement with our 24 hpf fate map analysis, dorsoventrally intermediate first-segment CNC contribute to the Pq cartilage.

Next, we made time-lapse recordings of *moz*⁻ second-segment skeletal development (Fig. 6B; see Movie 2 in the supplementary material). Consistent with previous analyses (Miller et al., 2004), we observe that the structure of the CNC segments at the beginning of the recordings is largely normal in *moz*⁻ animals. By the end of the recordings, we observe that dorsal CNC of the second segment do not form cartilage and instead a more ventral domain of CNC contributes to Pq'. In particular, by contrast to wild-type CNC, *moz*⁻ CNC along the dorsal portion of p1 fail to chondrify. To test if Moz controls chondrification cell-autonomously in CNC, we made time-lapse recordings of *moz*⁻ hosts in which a small number of transplanted wild-type CNC precursors populated the dorsal second segment (Fig. 6C; see Movie 3 in the supplementary material). The wild-type CNC along the dorsal portion of p1 expanded normally and formed cartilage in an otherwise *moz*⁻ environment (Fig. 6D). We conclude that Hox2 expression in zebrafish specifies the dorsal support skeleton by promoting, in a cell-autonomous manner, the expansion and chondrification of CNC adjacent to p1 endoderm.

Wild-type, but not *moz*⁻, second-segment cartilage requires p1 endoderm

As we saw a difference in cartilage potential of wild-type and *moz*⁻ CNC adjacent to p1, and as p1 is required for anterior Hm and Sy cartilages in wild types (Crump et al., 2004b), we asked whether p1 is required for the development of the jaw-like Pq' cartilage that replaces Hm and Sy in *moz*⁻ animals. In *itga5*^{b926} mutants, in which p1 fails to develop, second-segment-derived anterior Hm and Sy cartilage elements are selectively lost, yet the first-segment-derived Pq and M cartilages form normally (Fig. 7A-D) (Crump et al., 2004b). In our previous study (Crump et al., 2004b), the presence of the *fli1*:GFP transgene allowed us to select *itga5*^{b926} mutants in which p1 was absent. This live selection was crucial, as only *itga5*^{b926} mutants lacking p1 have subsequent cartilage loss. Thus, we used live selection to examine skeletal morphology in *moz*⁻*; itga5*^{b926}; *fli1*:GFP double mutants in which p1 was completely absent. In *moz*⁻*; itga5*^{b926}; *fli1*:GFP mutants lacking p1, the second-segment-derived Pq' and M' cartilages were similar in morphology to those in *moz* single mutants (Fig. 7G-J). However, we did observe increased fusions between Pq' and Pq in *moz*⁻*; itga5*^{b926} mutants,

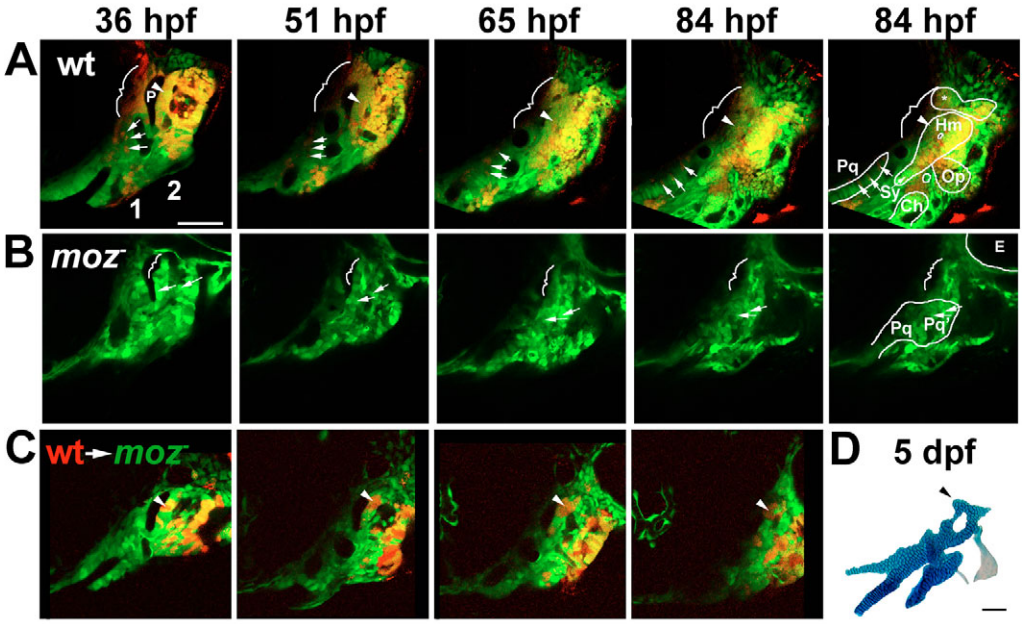

Fig. 6. Moz is required for the growth and chondrification of dorsal second-segment CNC. (**A**-**C**) Progressive frames, as indicated, from time-lapse confocal recordings of first (1) and second (2) pharyngeal segment development in wild-type *fli1*:GFP (A), *moz*⁻; *fli1*:GFP (B), and *moz*⁻; *fli1*:GFP/wild-type *fli1*:GFP mosaic (C) animals. Skeletal outlines are shown at 84 hpf. (**A**) A subset of CNC precursors are labelled with a red dye. In wild type (*n*=4), dorsal second-segment CNC (arrowheads) adjacent to p1 endoderm (P) form the anterior part of Hm cartilage. Dorsal first-segment CNC (brackets) form either no cartilage or neurocranial cartilage (*). Intermediate first-segment CNC (arrows) contribute to Pq cartilage. (**B**) In *moz*⁻; *fli1*:GFP animals (*n*=6), intermediate second-segment CNC contribute to Pq' cartilage (arrows). More dorsal CNC make no cartilage (brackets). In C, small amounts of wild-type CNC precursors (red) were transplanted into *moz*⁻; *fli1*:GFP animals. Wild-type second-segment CNC (arrowheads) adjacent to p1 grow and form a cartilage nodule in the normally cartilage-free dorsal zone of the *moz*⁻ host. (**D**) The skeletal preparation of this same animal at 5 dpf. Scale bars: 50 μm. See also Movies 1-3 in the supplementary material.

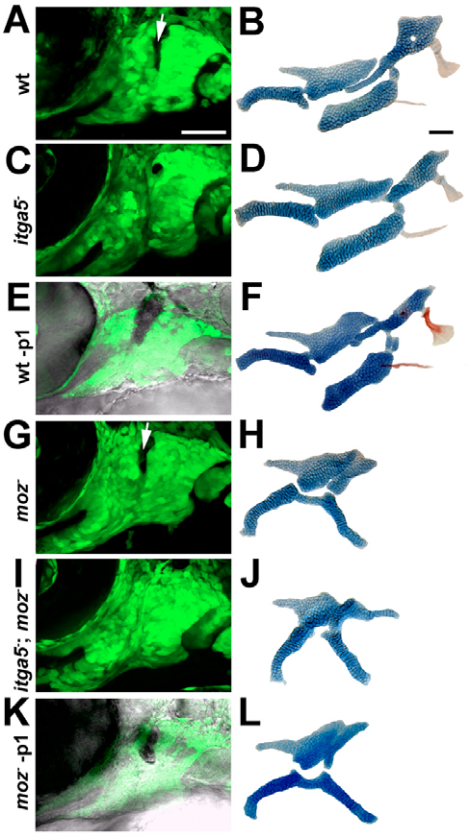

Fig. 7. The development of *moz*⁻ second-segment cartilage does not depend on p1 endoderm. CNC segments at 36 hpf (**A**,**C**,**E**,**G**,**I**,**K**) and facial skeletons at 4 dpf (**B**,**D**,**F**,**H**,**J**,**L**) from wild-type *fli1*:GFP (A,B,E,F), *itga5*^{b926}; *fli1*:GFP (C,D), *moz*⁻; *fli1*:GFP (G,H,K,L), and *moz*⁻; *itga5*^{b926}; *fli1*:GFP (I,J) animals. In E and K, inclusion of the Normarski channel shows that p1 endoderm has been selectively ablated by laser irradiation, as evinced by the dark pyknotic nuclei. When p1 is eliminated in either *itga5*^{b926}; *fli1*:GFP (C) or p1 ablated (–p1) (E) animals, the anterior portion of the Hm cartilage is lost and Sy cartilage is variably reduced (D,F). However, removal of p1 in *moz*⁻; *itga5*^{b926}; *fli1*:GFP (I) or p1 ablated *moz*⁻ (K) animals does not affect the shape of Pq′ (J,L). For p1 laser ablations, 13/14 wild-type animals had reduced Hm cartilage and 0/5 *moz* mutants had reduced Pq′. Arrows denote p1. Scale bars: 50 μm.

consistent with pouches also acting as barriers between the cartilage-forming CNC of neighbouring segments (Crump et al., 2004a; Piotrowski and Nusslein-Volhard, 2000). We also independently probed the requirement for p1 in wild-type and *moz*⁻ skeletal development by eliminating p1 with laser ablation. As with the genetic loss of p1, the laser ablation resulted in the loss of wild-type, but not *moz*⁻, second-segment skeletal derivatives (Fig. 7E,F,K,L). In conclusion, we find that, by contrast to normal second-segment derivatives, the duplicate jaw-like cartilages that form from *moz*⁻ second segments do not require p1 endoderm, and, by inference, must be responding to a different source of signals from those that induce the wild-type support skeleton.

DISCUSSION

Hox genes are CNC-intrinsic regulators of facial skeletal patterning

Since the discovery that Hox genes control anteroposterior identity in the facial skeleton (Gendron-Maguire et al., 1993; Rijli et al., 1993), Hox genes have largely been assumed to function within skeletal precursors to confer their distinct characters. Yet Hox genes also have limited expression in the ectoderm and endoderm that surround the skeletogenic CNC (this study) (Couly et al., 1998; Hunt et al., 1991; Maconochie et al., 1999). Indeed, misexpression studies suggest that *Hoxa2* confers regional identity on the ectoderm and endoderm and that this specification is important for inductive signalling to CNC (Couly et al., 1998; Grammatopoulos et al., 2000). By contrast, our mosaic analyses revealed a Hox2 skeletal patterning role only in CNC in *moz*⁻ and *hox2*-MO embryos, which lack *hoxa2b* and *hoxb2a* expression and function in all facial tissues: specific loss of Moz function in CNC gives homeotic skeletal transformations as severe as those seen in fully *moz*⁻ animals, and restoring Moz function specifically in CNC completely rescues *moz*⁻ support skeleton development. Moz probably acts through Hox2 genes, as we find that Moz controls Hox2 expression cell-autonomously in CNC, and wild-type CNC also completely rescue *hox2*-MO skeletal defects. Furthermore, as Moz is required for the maintenance of Hox2 expression in postmigratory CNC, but not for Hox expression in premigratory CNC, our *moz*⁻ CNC into wild-type mosaics demonstrate a late skeletal patterning function for Hox2 expression in postmigratory CNC. Recent experiments in mouse, in which *Hoxa2* function was eliminated specifically in postmigratory CNC, demonstrate that the late CNC-specific function of Hox2 genes in skeletal patterning is conserved from fish to mammals (Santagati et al., 2005).

We find that Moz-dependent Hox2 expression in CNC, in the absence of Hox2 expression in the endoderm and ectoderm, is entirely sufficient to generate a second-segment-derived support skeleton. The lack of a role for Hox2 genes in the ectoderm might seem to contradict previous experiments in avian and amphibian embryos (Couly et al., 1998; Creuzet et al., 2002; Grammatopoulos et al., 2000), showing that *Hoxa2* needs to be misexpressed throughout the embryo, not just in CNC, in order to induce the formation of second-segment skeletal derivatives from first-segment CNC. The results were interpreted to mean that CNC require a signal from *Hoxa2*-expressing ectoderm. Alternatively, it is known that first and second arch ectoderm differ in more than just Hox expression, e.g. *pitx2* expression, normally present in the first segment, does not turn on ectopically in the *moz*⁻ second segment (Miller et al., 2004). Strikingly, in mice, new elements (e.g. a pterygoquadrate-like cartilage) arise in the *Hoxa2*$^{-/-}$ second segment that do not form in the wild-type first segment (Rijli et al., 1993), suggesting that first and second arch epithelia (including the ectoderm) have different skeletal-inducing properties even in the absence of Hox2 expression. One possibility is that first, but not second, segment epithelium has an inhibitory influence on the development of Hox-expressing CNC. Our analyses would not detect such an influence, but the misexpression studies would. Nonetheless, our work shows that Hox2 expression in the ectoderm and endoderm is not required for the specification of second-segment skeletal derivatives.

Furthermore, our detailed expression analyses support the same conclusion. In the pharynx, only *hoxa2b* is expressed outside CNC, and it is expressed in very limited domains of first and second-segment ectoderm and endoderm. We detect no *hoxa2b* or *hoxb2a* expression in p1 endoderm, an epithelial domain that we have shown to be crucial for support skeleton development (Crump et al., 2004a; Crump et al., 2004b). Moreover, zebrafish *hoxa2b* and mouse *Hoxa2* are expressed in only a small domain of ectoderm at the first and second segment boundary (this study) (Hunter and Prince, 2002; Maconochie et al., 1999), and avian *Hoxa2* ectoderm expression is reported only in a small domain at the second and third segment boundaries (Couly et al., 1998). Thus, the lack of widespread Hox2

expression in second-segment ectoderm and endoderm is consistent with Hox2 genes not having skeletal patterning functions in second-segment epithelia. However, we stress that Hox genes probably have other functions in the facial ectoderm and endoderm, separate from skeletal patterning, that we have not addressed here. The facial ectoderm and pouch endoderm undergo complex patterns of morphogenesis that generate endocrine organs and gill elaborations (Hogan et al., 2004), and Hoxa3, for example, has been suggested to function in the endoderm for development of the thymus and parathyroid (Manley and Capecchi, 1998).

CNC-intrinsic factors regulate skeletogenesis in response to spatially restricted extrinsic signals

A longstanding debate is the extent to which extrinsic and intrinsic cues instruct facial skeletal patterning. Noden proposed that CNC are intrinsically 'prepatterned' (Noden, 1983; Trainor et al., 2002). By contrast, numerous studies suggest that extrinsic signals from the pharyngeal endoderm and oral ectoderm pattern the facial skeleton (Couly et al., 2002; Crump et al., 2004a; Crump et al., 2004b; Eberhart et al., 2006; Helms and Schneider, 2003; Piotrowski and Nusslein-Volhard, 2000; Ruhin et al., 2003). Hox genes determine segment-specific organ structure in diverse animals and have been assumed to pattern distinct 'identities' within sets of cells that begin development identically from segment to segment. However, our wild-type and *moz*$^{-}$ fate maps show that the CNC skeletal primordia are positionally non-equivalent in adjacent segments. Thus, Hox genes select which cells in a segment will make skeleton, rather than selecting what sort of skeleton comes from pre-specified cells.

How are these preskeletal CNC subsets selected? We show that Hox2 genes instruct CNC to respond to cues from particular local epithelia, one of which is p1 endoderm. Wild-type second-segment CNC along dorsal p1 form support cartilage, yet positionally equivalent wild-type first-segment, or *moz*$^{-}$ second-segment CNC, do not contribute to jaw-like cartilages. A few wild-type first-segment CNC and *moz*$^{-}$ second-segment CNC near ventral-medial p1 do in fact give rise to jaw and jaw-like cartilages. However, when p1 is genetically removed or laser ablated, jaw and jaw-like cartilages are not affected. Thus, even those non-Hox-expressing CNC close to p1 may not depend on p1 for their development.

In addition, a prominent feature of zebrafish *moz* mutants and mouse *Hoxa2* mutants is the mirror-image symmetry of the skeletal duplications, with the axis of symmetry at the boundary between the first and second segment. p1 endoderm, at this boundary, is clearly not responsible for mirror-image skeletal duplications, because jaw and jaw-like cartilages are unaffected by its absence. Furthermore, both the jaw and *moz*$^{-}$ jaw-like cartilages derive from intermediate and ventral segmental domains, whereas p1 is dorsal. Thus, there are probably additional segmental boundary epithelial signalling centres that account for the mirror-image symmetry. Medial endoderm (Fig. S1A) and *bmp4*-expressing ventral ectoderm are good candidates.

Wild-type cartilage precursors fate map close to endoderm, whereas dermal bone precursors develop adjacent to surface ectoderm. This segregation suggests a model in which endoderm locally induces cartilage fate and ectoderm induces dermal bone fate. Intriguingly, in *moz* mutants second-segment Op and Br dermal bones fail to form, yet we know from work on the *itga5*^{b926} mutant that dermal bone development does not depend on the presence of p1 endoderm (Crump et al., 2004b). Thus, Moz-dependent Hox expression probably controls the response of CNC to more than just p1 endoderm; signals to dermal bone precursors may come from the ectoderm (Tyler and Hall, 1977). In addition, there is considerable overlap between the wild-type and *moz*$^{-}$ fate maps in the ventral second segment, and thus differences between support and jaw skeletons may also arise by Hox2 genes controlling distinct morphogenetic behaviours of spatially equivalent CNC in the first two segments (O'Gorman, 2005).

In our model, postmigratory CNC encounter endodermal and ectodermal epithelia that have the ability to induce cartilage and bone differentiation in specific locations. Hox genes, functioning intrinsically, then instruct CNC to undergo skeletogenesis in response to a subset of these epithelia, thus positioning cartilage and dermal bone elements in the appropriate geometry. Our findings are consistent with avian grafting experiments showing that distinct domains of head endoderm control the shape and position of facial skeletal elements (Couly et al., 2002; Ruhin et al., 2003). These studies concluded that non-Hox-expressing and Hox-expressing CNC form separate equivalence groups, and that within these equivalence groups the type of skeleton can be reprogrammed by the type of grafted endoderm. However, the interaction might not be direct, as endoderm has a role at premigratory CNC stages, when the avian endoderm grafts were done, in patterning the facial ectoderm (Haworth et al., 2004), which is known to provide signals to skeletogenic CNC. In the future, the generation of p1-specific markers will allow us to test whether p1 endoderm is sufficient at postmigratory CNC stages to induce dorsal support cartilage in Hox-positive but not Hox-negative CNC. At the same time, it will be important to identify the downstream effectors of Hox2, and how this Hox2-dependent 'set' regulates the responses of CNC to specific epithelia.

We thank Craig T. Miller, Rob White, Cecilia Moens and Paul Trainor for comments; John Dowd and Jenny Lawson for fish care; and Poh Kheng Loi, Yi-Lin Yan and Adriana Rodriquez-Mari for help with in-situ sections. J.G.C. was an O'Donnell Fellow of the Life Sciences Research Foundation, and J.K.E. is an NIH postdoctoral fellow. Research is funded by NIH grants DE13834 and HD22486. The authors declare that they have no competing financial interests.

Supplementary material

Supplementary material for this article is available at http://dev.biologists.org/cgi/content/full/133/14/2661/DC1

References

Ando, R., Hama, H., Yamamoto-Hino, M., Mizuno, H. and Miyawaki, A. (2002). An optical marker based on the UV-induced green-to-red photoconversion of a fluorescent protein. *Proc. Natl. Acad. Sci. USA* **99**, 12651-12656.

Couly, G., Grapin-Botton, A., Coltey, P., Ruhin, B. and Le Douarin, N. M. (1998). Determination of the identity of the derivatives of the cephalic neural crest: incompatibility between Hox gene expression and lower jaw development. *Development* **125**, 3445-3459.

Couly, G., Creuzet, S., Bennaceur, S., Vincent, C. and Le Douarin, N. M. (2002). Interactions between Hox-negative cephalic neural crest cells and the foregut endoderm in patterning the facial skeleton in the vertebrate head. *Development* **129**, 1061-1073.

Creuzet, S., Couly, G., Vincent, C. and Le Douarin, N. M. (2002). Negative effect of Hox gene expression on the development of the neural crest-derived facial skeleton. *Development* **129**, 4301-4313.

Crump, J. G., Maves, L., Lawson, N. D., Weinstein, B. M. and Kimmel, C. B. (2004a). An essential role for Fgfs in endodermal pouch formation influences later craniofacial skeletal patterning. *Development* **131**, 5703-5716.

Crump, J. G., Swartz, M. E. and Kimmel, C. B. (2004b). An integrin-dependent role of pouch endoderm in hyoid cartilage development. *PLoS Biol.* **2**, E244.

Eberhart, J. K., Swartz, M. E., Crump, J. G. and Kimmel, C. B. (2006). Early Hedgehog signaling from neural to oral epithelium organizes anterior craniofacial development. *Development* **133**, 1069-1077.

Gendron-Maguire, M., Mallo, M., Zhang, M. and Gridley, T. (1993). Hoxa-2 mutant mice exhibit homeotic transformation of skeletal elements derived from cranial neural crest. *Cell* **75**, 1317-1331.

Grammatopoulos, G. A., Bell, E., Toole, L., Lumsden, A. and Tucker, A. S. (2000). Homeotic transformation of branchial arch identity after Hoxa2 overexpression. *Development* **127**, 5355-5365.

Haworth, K. E., Healy, C., Morgan, P. and Sharpe, P. T. (2004). Regionalisation

of early head ectoderm is regulated by endoderm and prepatterns the orofacial epithelium. *Development* **131**, 4797-4806.
Helms, J. A. and Schneider, R. A. (2003). Cranial skeletal biology. *Nature* **423**, 326-331.
Hogan, B. M., Hunter, M. P., Oates, A. C., Crowhurst, M. O., Hall, N. E., Heath, J. K., Prince, V. E. and Lieschke, G. J. (2004). Zebrafish gcm2 is required for gill filament budding from pharyngeal ectoderm. *Dev. Biol.* **276**, 508-522.
Hombria, J. C. and Lovegrove, B. (2003). Beyond homeosis–HOX function in morphogenesis and organogenesis. *Differentiation* **71**, 461-476.
Hunt, P., Gulisano, M., Cook, M., Sham, M. H., Faiella, A., Wilkinson, D., Boncinelli, E. and Krumlauf, R. (1991). A distinct Hox code for the branchial region of the vertebrate head. *Nature* **353**, 861-864.
Hunter, M. P. and Prince, V. E. (2002). Zebrafish hox paralogue group 2 genes function redundantly as selector genes to pattern the second pharyngeal arch. *Dev. Biol.* **247**, 367-389.
Lawson, N. D. and Weinstein, B. M. (2002). In vivo imaging of embryonic vascular development using transgenic zebrafish. *Dev. Biol.* **248**, 307-318.
Le Douarin, N. M. (1982). *The Neural Crest*. Cambridge: Cambridge University Press.
Lyons, D. A., Guy, A. T. and Clarke, J. D. (2003). Monitoring neural progenitor fate through multiple rounds of division in an intact vertebrate brain. *Development* **130**, 3427-3436.
Maconochie, M., Krishnamurthy, R., Nonchev, S., Meier, P., Manzanares, M., Mitchell, P. J. and Krumlauf, R. (1999). Regulation of Hoxa2 in cranial neural crest cells involves members of the AP-2 family. *Development* **126**, 1483-1494.
Manley, N. R. and Capecchi, M. R. (1998). Hox group 3 paralogs regulate the development and migration of the thymus, thyroid, and parathyroid glands. *Dev. Biol.* **195**, 1-15.
Miller, C. T., Maves, L. and Kimmel, C. B. (2004). moz regulates Hox expression and pharyngeal segmental identity in zebrafish. *Development* **131**, 2443-2461.
Noden, D. M. (1983). The role of the neural crest in patterning of avian cranial skeletal, connective, and muscle tissues. *Dev. Biol.* **96**, 144-165.
O'Gorman, S. (2005). Second branchial arch lineages of the middle ear of wild-type and Hoxa2 mutant mice. *Dev. Dyn.* **234**, 124-131.
Pasqualetti, M., Ori, M., Nardi, I. and Rijli, F. M. (2000). Ectopic Hoxa2 induction after neural crest migration results in homeosis of jaw elements in Xenopus. *Development* **127**, 5367-5378.
Piotrowski, T. and Nusslein-Volhard, C. (2000). The endoderm plays an important role in patterning the segmented pharyngeal region in zebrafish (Danio rerio). *Dev. Biol.* **225**, 339-356.
Rijli, F. M., Mark, M., Lakkaraju, S., Dierich, A., Dolle, P. and Chambon, P. (1993). A homeotic transformation is generated in the rostral branchial region of the head by disruption of Hoxa-2, which acts as a selector gene. *Cell* **75**, 1333-1349.
Rodriguez-Mari, A., Yan, Y. L., Bremiller, R. A., Wilson, C., Canestro, C. and Postlethwait, J. H. (2005). Characterization and expression pattern of zebrafish Anti-Mullerian hormone (Amh) relative to sox9a, sox9b, and cyp19a1a, during gonad development. *Gene Expr. Patterns* **5**, 655-667.
Ruhin, B., Creuzet, S., Vincent, C., Benouaiche, L., Le Douarin, N. M. and Couly, G. (2003). Patterning of the hyoid cartilage depends upon signals arising from the ventral foregut endoderm. *Dev. Dyn.* **228**, 239-246.
Santagati, F., Minoux, M., Ren, S. Y. and Rijli, F. M. (2005). Temporal requirement of Hoxa2 in cranial neural crest skeletal morphogenesis. *Development* **132**, 4927-4936.
Schilling, T. F. and Kimmel, C. B. (1994). Segment and cell type lineage restrictions during pharyngeal arch development in the zebrafish embryo. *Development* **120**, 483-494.
Trainor, P. A., Ariza-McNaughton, L. and Krumlauf, R. (2002). Role of the isthmus and FGFs in resolving the paradox of neural crest plasticity and prepatterning. *Science* **295**, 1288-1291.
Tyler, M. S. and Hall, B. K. (1977). Epithelial influences on skeletogenesis in the mandible of the embryonic chick. *Anat. Rec.* **188**, 229-239.